



Significant vertical water transport by mountain-induced circulations on Mars

T. I. Michaels,¹ A. Colaprete,² and S. C. R. Rafkin¹

Received 11 April 2006; revised 19 May 2006; accepted 12 July 2006; published 16 August 2006.

[1] Using a 3-D, non-hydrostatic mesoscale Mars atmospheric model with detailed aerosol/cloud microphysics, we show that the formation of discrete afternoon clouds over the Olympus Mons volcano is due to the symbiosis of upslope thermal flow and a lee mountain wave circulation, and that these clouds exhibit complex particle distributions. Furthermore, we illustrate that this and other mountain-induced circulations transport large quantities of dust, water vapor, and water ice aerosol from lower altitudes into the free atmosphere general circulation. Therefore, these circulations are an important part of Mars' net Hadley circulation and climatic forcing. **Citation:** Michaels, T. I., A. Colaprete, and S. C. R. Rafkin (2006), Significant vertical water transport by mountain-induced circulations on Mars, *Geophys. Res. Lett.*, 33, L16201, doi:10.1029/2006GL026562.

1. Introduction

[2] Observational studies of data returned by the Mariner 6 and 7 flyby spacecraft [Peale, 1973; Smith and Smith, 1972], the Mariner 9 orbiter [Leovy et al., 1973; Hartmann, 1978], the dual Viking orbiters [Kahn, 1984], the Hubble Space Telescope [James et al., 1996], and the Mars Orbiter Camera (MOC) aboard the Mars Global Surveyor (MGS) spacecraft [Benson et al., 2003] reveal that all four primary Tharsis volcanoes (Olympus Mons, Ascraeus Mons, Pavonis Mons, and Arsia Mons) are seasonally associated with relatively discrete, bright, and optically thick clouds that are “anchored” with respect to the underlying topography. Often first appearing in late morning above their summit calderas, the clouds increase in areal extent and brightness with time, ultimately becoming horizontal “plumes” stretching westward for up to several hundred kilometers by mid-afternoon. Data from the Mariner 9 infrared spectrometer demonstrate that these clouds are likely composed of water ice crystals only microns in diameter [Curran et al., 1973].

[3] It is widely believed that these clouds form in response to upward vertical motion induced by each volcano within a relatively moist and dust-laden atmospheric environment [e.g., Benson et al., 2003]. Previous works have mentioned that thermally-driven slope flow is likely an influential component of this vertical motion [e.g., Clancy et al., 1996], although other distinct types of atmospheric circulations (i.e., mountain waves, “barrier” uplift) may

also have significant roles. Further details about these clouds (e.g., particle size distribution, three-dimensional morphology, time evolution, climatic role) are poorly constrained or largely unknown, due to the paucity of appropriate observations. Fortunately, the above details may be recovered or constrained using appropriate three-dimensional numerical atmospheric models suitably validated against observations.

[4] Qualitative comparison with the winds predicted by a Mars general circulation model (MGCM; global model) [Haberle et al., 1993] reveals that the cloud “plumes” are oriented directly downwind of the volcanoes and have an extent roughly consistent with the distance the general circulation would have transported material downstream since late morning. MGCMs with simplified aerosol/cloud microphysics [e.g., Richardson et al., 2002] often form significant water ice clouds in the lee of Olympus Mons that are qualitatively similar to observations. However, current MGCMs (with a typical grid cell size $>4 \times 4$ degrees in latitude/longitude) resolve Olympus Mons (and its associated atmospheric circulations) only marginally at best, and therefore are poorly suited for investigating the detailed formation processes and nature of these discrete clouds. A mesoscale (typical grid cell size <100 km) model (ideally with detailed aerosol/cloud microphysics) is more appropriately suited for the investigation of these clouds.

[5] Recent MGCM studies successfully simulated the broad global-scale temporal and spatial distribution of water-ice clouds, and concluded that most water ice clouds, in addition to airborne dust, are climatologically important on Mars [Richardson et al., 2002; Montmessin et al., 2004]. Thus any process that significantly enhances or reduces the extent of such clouds or dust (either directly or indirectly) is also climatologically important. Another MGCM study [Hinson and Wilson, 2004] revealed a modulating feedback between thermal atmospheric tides and the regional-scale water-ice clouds of Tharsis and the Martian tropics (at least during the northern hemisphere mid-summer). Furthermore, their modeling results indicated a significant diurnal cycle in cloud extent and thickness over the Tharsis region.

[6] The presence of relatively thick afternoon mid-level water-ice clouds associated with the large volcanoes of Mars (such as Olympus Mons) in northern spring and summer implies the presence of upward vertical water and dust transport induced by the extreme topography. This work uses a mesoscale atmospheric model with detailed aerosol/cloud microphysics to comprehensively investigate the mechanisms of cloud formation and the transport of dust, water vapor, and condensate over the Olympus Mons volcano. This modeling enables for the first time an assessment of the effect that these mountain-induced processes have on

¹Department of Space Studies, Southwest Research Institute, Boulder, Colorado, USA.

²NASA Ames Research Center, Moffett Field, California, USA.

the general circulation and the global dust and hydrologic cycles.

2. Model and Experiment

[7] The atmospheric model employed in the present study is the Mars Regional Atmospheric Modeling System (MRAMS), which is a mesoscale, three-dimensional model that numerically solves the non-hydrostatic, fully compressible momentum, continuity, and thermodynamic equations to simulate the atmosphere [Rafkin *et al.*, 2001]. For this investigation, MRAMS was coupled to a detailed, time-dependent aerosol/cloud microphysics model. A simpler microphysical model was not used because of the known sensitivity of MGCM results to the choice of simplified cloud scheme used, largely because of differing assumptions and approximations [Richardson *et al.*, 2002; Montmessin *et al.*, 2004]. In order to minimize this issue, the microphysical model used in this study has minimal assumptions and approximations [Colaprete *et al.*, 1999], and discretizes the mass (size) distributions of dust and water ice aerosol particles into bins (8 dust bins from 0.05–5 μm ; 18 water-ice bins from 0.07–102 μm). All modeled aerosol particles are subject to the full range of atmospheric transport, including gravitational settling (precipitation) and turbulent mixing. Water ice is permitted to heterogeneously nucleate (and then deposit/sublimate) on the explicitly modeled airborne dust. The coupling of this microphysical code with MRAMS permits the detailed investigation of cloud formation on Mars by explicitly modeling the evolution of the water-ice and dust particle size distributions. Additionally, all aerosol particles are treated as being radiatively active, using a two-stream radiative transfer algorithm.

[8] A series of three nested computational grids, each with a successively smaller total area and horizontal grid-spacing, were used to achieve the desired spatial resolution of approximately 40 km in the region of interest (the Tharsis Montes). The NASA Ames MGCM with relatively simple cloud microphysics [Colaprete and Haberle, 2001] provided MRAMS with its initial state and time-dependent boundary conditions. The mesoscale model was then run for several sols (i.e., Mars-days; ending at $L_s \simeq 100^\circ$) until a relatively stable diurnal cycle of cloud development was achieved.

3. Results and Discussion

[9] A comparison of MOC imagery (Figure 1a) with MRAMS results (Figure 1b) reveals much similarity. At this season Ascræus and Olympus Mons exhibit thick afternoon clouds over their western flanks (lee side), whereas Pavonis and Arsia Mons have little or no optically thick cloud. Thermal Emission Spectrometer (TES) water vapor column abundance maps [Smith, 2004] indicate that at this season, only Ascræus and Olympus Mons have relatively abundant water vapor in their vicinity (this is also the case in the MRAMS initial condition). Correspondingly, the shape, orientation, and qualitative opacity of the simulated clouds associated with Ascræus and Olympus Mons are quite similar to those seen by the MOC. Note that the nested grid structure and model spinup period used here, the short radiative time constant of Mars' atmosphere, and strong topographic control of regional circulations significantly

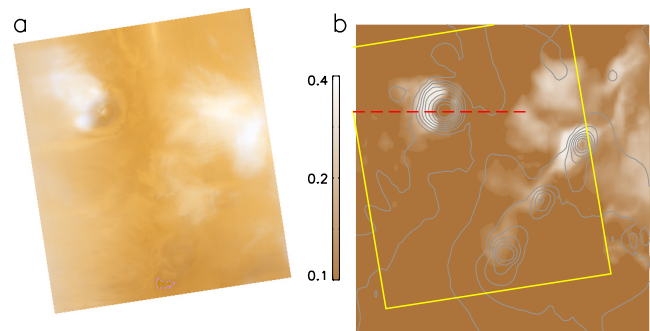


Figure 1. Clouds over the Tharsis volcanoes ($L_s \simeq 100^\circ$, ~ 1345 LST at Arsia Mons). (a) Portion of composite color MOC wide-angle imagery (M23-00630&1; blue & red filter channels, green \simeq (blue + red)/2). (b) MRAMS water-ice cloud total column opacity in the 400–800 nm spectral band (white shading), with model topography (contoured gray; interval is 2.4 km) for reference. The approximate location/orientation of the MOC image (yellow lines), and the location of the cross-section shown in Figure 2 (red dashed line) are also indicated.

reduce the influence of the MGCM initial state on the MRAMS results. Even so, differences between the real-world state (“weather”) and the *probable* state computed by models (“climate”) are possible (e.g., the thin cloud over Arsia Mons that is only present in the MRAMS solution). Bolstered by the very good qualitative agreement between the modeled and observed clouds, the dynamics and microphysics of the clouds simulated by the model are taken as a realistic numerical representation of natural cloud formation.

[10] The model results show that the Olympus Mons afternoon clouds are due primarily to a symbiosis between thermally-induced upslope flow (anabatic wind) and the rising branch of a mountain (gravity) wave. The combined lee side updraft extends from the base of the volcano to >15 km above the caldera (Figure 2a), and primarily acts to transport water vapor- and dust- laden air parcels from lower levels. Just below the volcano’s peak (where the blocking effect of the mountain is greatly reduced), the terrain-following updraft air parcel trajectories begin to be deflected westward into a dynamically-maintained region of sharply depressed temperature (up to 10 K deviation), producing a primary cloud particle growth region (CGR1) that persists throughout the late morning and afternoon. Cloud particle production also occurs well above the level of the caldera (CGR2), but the water vapor and dust involved primarily originates aloft on the windward side. An additional cloud formation region, manifested as a cloud arc windward of the summit caldera, is strongly modulated and nearly suppressed entirely by subsident flow (due to both mountain wave dynamics and “return” flow associated with the lee upslope flow).

[11] A wide variety of cloud particle populations is present in the model results. Rapid growth in water-rich CGR1 and water-poor CGR2 results in narrow distributions of water-ice particles with relatively large ($r_{\text{eff}} \simeq 8 \mu\text{m}$) and small ($r_{\text{eff}} \simeq 2 \mu\text{m}$) effective radii, respectively. The CGR1 effective radius is consistent with telescopic spectral determinations of Elysium Mons afternoon cloud particles [Glenar *et al.*, 2003], while the CGR2 particle size is similar

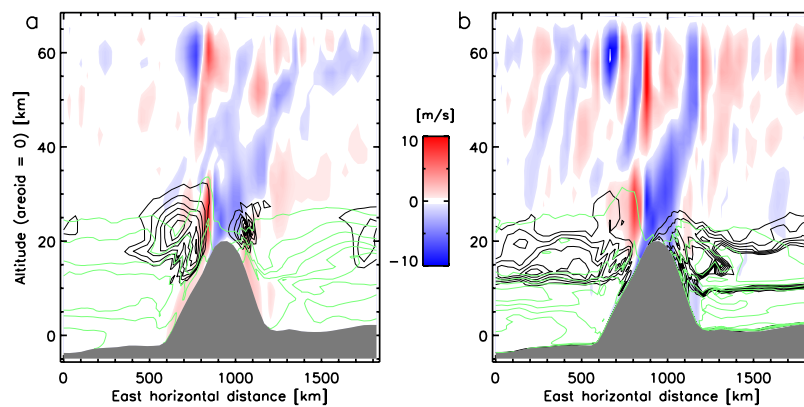


Figure 2. MRAMS instantaneous vertical W-E cross-sections (topography shaded gray) through the Olympus Mons summit, with vertical velocity shaded in blue (down) and red (up), and contours of cloud water-ice mass mixing ratio (black; 1×10^{-5} to 5.17×10^{-5}) and water vapor mass mixing ratio (green; 1×10^{-5} to 1.18×10^{-4}). (a) Afternoon (2240 UT; \sim 1340 LST), showing discrete clouds and upslope flow along the volcano’s flanks. (b) Night (1100 UT; \sim 0200 LST), showing downslope flow and a pronounced lee mountain wave.

to the TES-derived results of *Wolff and Clancy* [2003]. As they form, these particles are transported downstream (to the west) and out of the updraft core by the large-scale horizontal winds. A substantial portion of the cloud mass quickly falls to lower elevations above the volcano’s flank (the larger particles, with fall velocities $\sim 1 \text{ m s}^{-1}$), but the smaller particles have settling times long enough to create a cloud “plume” downstream (Figures 1 and 2a), which elongates with time. Preferential sedimentation of larger particles results in size sorting within the plume such that the effective condensate particle radius generally decreases with both height and lateral distance from the volcano. Rapid, often turbulent transport of diverse water-ice particle distributions (especially in the lee, just above and below the most massive portions of the cloud) creates multiple regions of bimodal particle distributions.

[12] The simulated particle size and spatial distributions are clearly in conflict with simple microphysical representations used in some models [e.g., *Richardson et al.*, 2002], and also with TES retrievals of aerosol effective radius that assume that particle sizes are constant with height [e.g., *Wolff and Clancy*, 2003]. Therefore, the magnitude of the effect of these significant spatial and temporal variations of aerosol size distributions should be considered when interpreting radiance-derived and model-predicted fields that are based on simpler assumptions about aerosol size and spatial distributions.

[13] The lee cloud extends from ~ 10 – 35 km , nearly 10 km higher than the preexisting layer of relatively high water vapor content (Figure 2a). This indicates that the daytime volcano-induced circulations not only cause some water vapor in the large-scale layer to condense, but also transport (“pump”) the water ice mass to altitudes it otherwise could not attain. At night (Figure 2b), widespread cooling within the upper half of the moist layer creates a regional water-ice cloud “shield” ($r_{\text{eff}} \simeq 6.5 \mu\text{m}$) that persists until morning. The horizontal extent and location of this nocturnal cloud deck compares well with that inferred from MOLA radiometry [*Neumann and Wilson*, 2006]. In the lee of Olympus Mons a strong mountain wave dominates, but is not properly juxtaposed with the moisture field and is therefore unable to significantly enhance the

nocturnal clouds. Instead, the warm sector of the wave sublimates adjacent portions of the nocturnal cloud “shield”, then vertically transports the resulting water vapor and dust mass upward to altitudes greater than 40 km . At all times of day, therefore, Olympus Mons circulations vertically transport large amounts of water, dust, and air mass.

[14] The net upward air and aerosol transport achieved each sol by Ascraeus and Olympus Mons is demonstrated by their net areal mass flux (i.e., the net rate of mass flow through a given area over one sol) vertical profiles (Figures 3a–3c), which include vertical air velocity and (where relevant) particle fall velocity transport terms. The areal flux of air (Figure 3a) is strongly positive (upward) to $\sim 25 \text{ km}$, above which (to $\sim 45 \text{ km}$) compensating subsidence is dominant. The Ascraeus areal flux profile of total water substance (Figure 3b) shows net upward transport at nearly all heights, but has a shape that implies water depletion below $\sim 12 \text{ km}$, and the addition of water mass above that (Figure 3c) - a water pump. The Olympus water flux profiles are similar, though they exhibit two regions of strong upward flux, separated by a weak region of downward flux at $\sim 12 \text{ km}$. Also, dust is transported upward nearly everywhere (Figure 3b, red). It is also important to note that significant horizontal transport is occurring simultaneously with this vertical transport at levels $> 15 \text{ km}$, effectively extending the impact of each mountain-induced pump to regional, and possibly even global scales. This is consistent with the earlier findings of dust transport by Arsia Mons [*Rafkin et al.*, 2002].

[15] Integrating the total water substance net flux profiles with height for both volcanoes (using MRAMS results) and an entire latitude belt (7.5 – 22.5°N ; using MGCM results) yields net column flux values that may then be compared. The total water substance flux predicted by MRAMS over Ascraeus and Olympus Mons can account for fully one-third (a column-integrated value of $1.9 \text{ kg sol}^{-1} \text{ m}^{-2} \text{ m}$) of the vertical water transport done by the MGCM Hadley cell (the Tharsis volcanoes are not individually resolved) over the entire latitude belt. Such mountain-induced circulations are thus an important facet of the global water cycle, and possibly the dust cycle as well. This indicates that one longitudinal asymmetry in the MGCM Hadley cell water

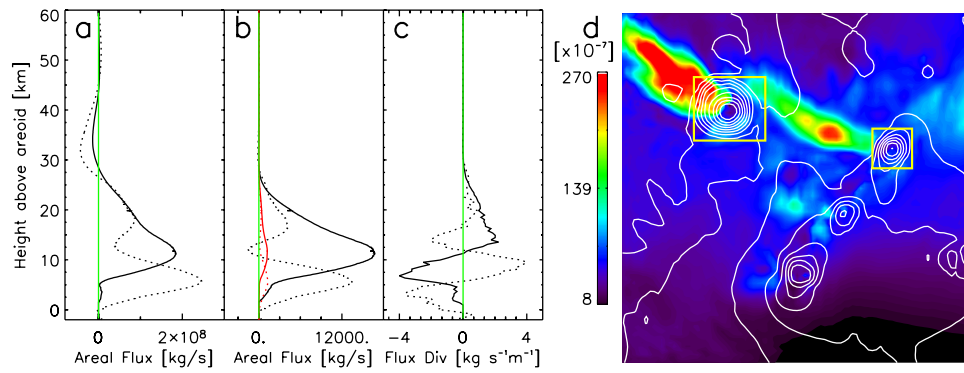


Figure 3. Illustrations of the time-average (over 1 sol; green lines reference zero) atmospheric pumps induced by Ascræus Mons (solid profiles) and Olympus Mons (dotted profiles), and also the instantaneous enrichment of their environment (areas used to calculate the time-average profiles outlined in yellow). (a) Areal flux profiles for dry air. (b) Areal flux profiles for total water substance (vapor + ice; black), and total dust substance (free dust + that within water-ice cloud particles; red). (c) Profiles of the areal flux convergence of the total water substance. (d) Instantaneous (1600 UT; ~0800 LST at Arsia Mons) plot of plumes of relatively large total water substance mass mixing ratio (color shading) on a constant areopotential surface of 43.5 km. Model topography is shown for reference (white contours).

transport (dominant/enhanced rising branch over the Tharsis region) may in reality be substantially due to these volcano-induced circulations. Furthermore, above about 40 km, these volcanoes introduce large, daily plumes of water and dust that have mass mixing ratios more than two orders of magnitude larger than the surrounding regional environment (Figure 3d). Such injection into the higher reaches of the atmosphere may produce many of the high-altitude (>40 km) dust and thin cloud layers seen on Mars' limb by spacecraft [e.g., *Jaquin et al.*, 1986], as well as possible (but as of yet unobserved) high-altitude layers of water vapor. The Mars Express and Mars Reconnaissance Orbiter spacecraft may be able to confirm the presence of these elevated aerosol and vapor layers if they exist. These circulations may be a significant mechanism for maintaining the global atmospheric dust load above ~10 km (i.e., above the boundary layer, in the free atmosphere), since other vertical dust-transport mechanisms in the free atmosphere are much slower (e.g., Hadley cell transport).

[16] Relatively rapid, localized aerosol and moisture enrichment of the higher reaches of the free atmosphere by vertical circulations rooted near the surface is highly analogous to some effects of terrestrial thunderstorms. Even though these Martian circulations and terrestrial thunderstorms have different primary energy sources (differential solar heating vs. condensational latent heating), both result in relatively localized enrichment of aerosols and water vapor in the free atmosphere. On Earth, deep penetrative moist convection in the form of relatively discrete thunderstorms, rather than the mean motion of the rising branch of the *statistical* meridional circulation known as the Hadley cell, is the primary mechanism for vertical energy (moisture) transport in the tropical atmosphere [*Riehl and Malkus*, 1958; *Riehl and Simpson*, 1979]. As the mountain-induced circulations of Olympus Mons and other tropical zone volcanoes are discrete (i.e., areal extent is small compared with the total area of the tropics), rapid transport mechanisms for moisture and aerosols, the above analogy may thus be further extended to general circulation effects: we suggest that these mountain-induced circulations are an essential part of Mars' global atmospheric energy budget, and play

important roles in the dust cycle, water cycle, and the cycles of other chemical species that are significantly affected by rapid vertical transport through the lowest several scale heights of the atmosphere.

4. Concluding Remarks

[17] In summary, we utilized a mesoscale atmospheric model (MRAMS) with sophisticated aerosol/cloud microphysics to investigate the cloud formation and circulations that Olympus Mons and other Mars volcanoes induce in early northern hemisphere summer ($L_s \simeq 100^\circ$). MRAMS simulations are found to qualitatively reproduce observed cloud locations, orientations, and morphologies well. The formation of discrete afternoon clouds over Olympus Mons is shown to be due to the symbiosis of upslope thermal flow and a lee mountain wave circulation. We further illustrate that these two mountain-induced atmospheric circulations (thermally-driven slope flows and mountain waves) cause the vertical transport of water substance throughout each Mars day. We find that the daily net effect of the circulations induced by Ascræus and Olympus Mons at this season is to pump large quantities of water vapor, water ice aerosol, and dust upward from lower levels, injecting the said material into the free atmosphere general circulation, where it may be further transported globally. Furthermore, these mountain-induced circulations may be a significant (perhaps primary) mechanism for injecting water, dust, and other aerosols above 40 km in altitude. Finally, the effects of the atmospheric circulations induced by large mountains on Mars are found to be analogous to terrestrial thunderstorms in many ways, including being an important part of Mars' net Hadley circulation (and therefore the atmospheric water and dust cycles), and thus are climatologically significant.

[18] **Acknowledgment.** This work was supported by NASA under the Mars Data Analysis Program (MDAP) and the Planetary Atmospheres program (PATM; NNG05GB50G).

References

Benson, J. L., et al. (2003), The seasonal behavior of water ice clouds in the Tharsis and Valles Marineris regions of Mars: Mars Orbiter Camera observations, *Icarus*, 165, 34–52.

- Clancy, R. T., et al. (1996), Water vapor saturation at low altitudes around Mars aphelion: A key to Mars climate, *Icarus*, *122*, 36–62.
- Colaprete, A., and R. M. Haberle (2001), A comparison of Mars GCM cloud simulations with observations, *Eos Trans. AGU*, *82*(47), Fall Meet. Suppl., P31A-0534.
- Colaprete, A., O. B. Toon, and J. A. Magalhães (1999), Cloud formation under Mars Pathfinder conditions, *J. Geophys. Res.*, *104*, 9043–9054.
- Curran, R. J., et al. (1973), Mars: Mariner 9 spectroscopic evidence for H₂O ice clouds, *Science*, *182*, 381–383.
- Glenar, D. A., et al. (2003), Spectral imaging of Martian water ice clouds and their diurnal behavior during the 1999 aphelion season ($L_s = 130^\circ$), *Icarus*, *161*, 297–318.
- Haberle, R. M., J. B. Pollack, J. R. Barnes, R. W. Zurek, C. B. Leovy, J. R. Murphy, H. Lee, and J. Schaeffer (1993), Mars atmospheric dynamics as simulated by the NASA Ames General Circulation Model. 1. The zonal-mean circulation, *J. Geophys. Res.*, *98*, 3093–3123.
- Hartmann, W. K. (1978), Mars—Topographic control of clouds, *Icarus*, *33*, 380–387.
- Hinson, D. P., and R. J. Wilson (2004), Temperature inversions, thermal tides, and water ice clouds in the Martian tropics, *J. Geophys. Res.*, *109*, E01002, doi:10.1029/2003JE002129.
- James, P. B., J. F. Bell III, R. T. Clancy, S. W. Lee, L. J. Martin, and M. J. Wolff (1996), Global imaging of Mars by Hubble space telescope during the 1995 opposition, *J. Geophys. Res.*, *101*, 18,883–18,890.
- Jaquin, F., P. Gierasch, and R. Kahn (1986), The vertical structure of limb hazes in the Martian atmosphere, *Icarus*, *68*, 442–461.
- Kahn, R. (1984), The spatial and seasonal distribution of Martian clouds and some meteorological implications, *J. Geophys. Res.*, *89*, 6671–6688.
- Leovy, C. B., G. A. Briggs, and B. A. Smith (1973), Mars atmosphere during the Mariner 9 extended mission: Television results, *J. Geophys. Res.*, *78*, 4252–4266.
- Montmessin, F., F. Forget, P. Rannou, M. Cabane, and R. M. Haberle (2004), Origin and role of water ice clouds in the Martian water cycle as inferred from a general circulation model, *J. Geophys. Res.*, *109*, E10004, doi:10.1029/2004JE002284.
- Neumann, G. A., and R. J. Wilson (2006), Night and day: The opacity of clouds measured by the Mars Orbiter Laser Altimeter (MOLA), *Lunar Planet. Sci.* [CD-ROM], XXXVII, Abstract 2330.
- Peale, J. S. (1973), Water and the Martian W cloud, *Icarus*, *18*, 497.
- Rafkin, S. C. R., R. M. Haberle, and T. I. Michaels (2001), The Mars Regional Atmospheric Modeling System: Model description and selected simulations, *Icarus*, *151*, 228–256.
- Rafkin, S. C. R., M. R. V. Sta. Maria, and T. I. Michaels (2002), Simulation of the atmospheric thermal circulation of a Martian volcano using a mesoscale numerical model, *Nature*, *419*, 697–699.
- Richardson, M. I., R. J. Wilson, and A. V. Rodin (2002), Water ice clouds in the Martian atmosphere: General circulation model experiments with a simple cloud scheme, *J. Geophys. Res.*, *107*(E9), 5064, doi:10.1029/2001JE001804.
- Riehl, H., and J. S. Malkus (1958), On the heat balance in the equatorial trough zone, *Geophysica*, *6*, 503–538.
- Riehl, H., and J. M. Simpson (1979), The heat balance of the equatorial trough zone, revisited, *Contrib. Atmos. Phys.*, *52*, 287–305.
- Smith, M. D. (2004), Interannual variability in TES atmospheric observations of Mars during 1999–2003, *Icarus*, *167*, 148–165.
- Smith, M. D., and B. A. Smith (1972), Diurnal and seasonal behavior of discrete white clouds on Mars, *Icarus*, *16*, 509–521.
- Wolff, M. J., and R. T. Clancy (2003), Constraints on the size of Martian aerosols from Thermal Emission Spectrometer observations, *J. Geophys. Res.*, *108*(E9), 5097, doi:10.1029/2003JE002057.

A. Colaprete, NASA Ames Research Center, MS 245-3, Moffett Field, CA 94035, USA. (anthony.colaprete-1@nasa.gov)

T. I. Michaels and S. C. R. Rafkin, Department of Space Studies, Southwest Research Institute, 1050 Walnut St., Suite 400, Boulder, CO 80302, USA. (tmichael@boulder.swri.edu)